

A data variation robust learning model based on importance sampling

Jiangshe Zhang*, Lizhen Ji, Fei Gao, Mengyao Li

School of Mathematics and Statistics, Xi'an Jiaotong University, No.28, Xianning West Road, Xi'an, Shannxi, 710049, P.R. China

Abstract

A crucial assumption underlying the most current theory of machine learning is that the training distribution is identical to the testing distribution. However, this assumption may not hold in some real-world applications. In this paper, we propose an importance sampling based data variation robust loss (ISloss) for learning problems which minimizes the worst case of loss under the constraint of distribution deviation. The distribution deviation constraint can be converted to the constraint over a set of weight distributions centered on the uniform distribution derived from the importance sampling method. Furthermore, we reveal that there is a relationship between ISloss under the logarithmic transformation (LogISloss) and the p-norm loss. We apply the proposed LogISloss to the face verification problem on Racial Faces in the Wild dataset and show that the proposed method is robust under large distribution deviations.

Keywords: , importance sampling, minimax principle, face verification

1. Introduction

A crucial assumption underlying the most current theory of machine learning is that the distribution of training samples is identical to the distribution of future test samples and we have obtained a lot of theoretical results based on this assumption, but it is often violated in practice where the distribution of future data deviates from the distribution

*Corresponding author

Email address: jszhang@mail.xjtu.edu.cn (Jiangshe Zhang)

of training data, and we must develop models that work well under realistic violations of this assumption. While the distribution of future data is unknown and a learning system learns only from distribution of the current training data, we cannot guarantee the strong performance of the trained system over the future system. In this paper, we will develop a data variation robust learning model based on importance sampling (IS-DVR) to deal with this problem. Here, *robust* means reliability with regard to distribution deviation of future testing data from current training data. Although we have considerable freedom in quantizing performance and deviation[13, 6, 14], we use Kullback–Leibler divergence[7, 29] to measure deviation of a future data distribution from the current data distribution.

The proposed IS-DVR model aims to minimize the loss in maximum degradation for a given deviation level. Maximum degradation of performance possible for a given deviation level is used to measure negative robustness, and an optimally robust model then minimizes this maximum degradation, and hence the corresponding optimization problem is a minimax problem[3]. Inspired from the importance sampling method[4, 18], we convert the constraint between the current distribution and future distribution to a constraint on the importance sampling weights. Then, we use the Lagrange method to reformulate the constrained minimax optimization problem into an unconstrained minimum optimization problem. The resulting objective function of the optimization problem is called Importance Sampling loss(**ISloss**). A logarithmic transformation of ISloss is called **LogISloss**.

Our proposed importance sampling based loss can be applied to many real-world applications where a future testing distribution deviates from the current training distribution. In this paper, we validate the effectiveness of our proposed algorithm on the face verification task. Face verification is one of the most popular topics in the community of computer vision and pattern recognition. It is a technology used to determine whether a pair of images belong to the same individual and is widely used for identity authentication in many areas such as attendance, finance, security, military, self-service and other fields. For example, installing face verification systems in schools and enterprises can check work attendance; applying facial verification software to ATMs can protect account safety from intruders

and identity thieves; using face verification technology in mobile phone APPs and computer applications can provide further security when logging into accounts. Compared with other biometric identification techniques such as fingerprinting and retina scanning, face verification system is of lower cost since it only uses a digital camera and does not require human contact, therefore it is widely used today. In the face verification community, researchers have proposed large-margin softmax variants [10, 9, 21, 2, 20, 22, 27, 8] to enhance the inter-class discrepancy and intra-class compactness, ArcMargin[2] and AddMargin[20, 22] are two widely-used ones. In this paper, we denote the cross-entropy loss(CEloss) under ArcMargin and AddMargin as ArcLoss and AddLoss. To validate the effectiveness of the proposed model, we apply LogISloss to ArcLoss and AddLoss and the resulting models are denoted as IS-ArcLoss and IS-AddLoss respectively. We conduct experiments with respect to distribution deviations and hardest pairs on Racial Faces in the Wild datasets(RFW)[11, 23, 24, 25, 26]. Experiment results on distribution deviations show that the learned features under LogISloss generalize well across different races and across different datasets compared with cross-entropy loss. Experiment results on the hardest pairs show that IS-ArcLoss attains higher cosine similarities on hard positive pairs and attains lower cosine similarities on hard negative pairs compared with ArcLoss, which indicates that IS-ArcLoss performs better on the hardest pairs.

Outline of the paper Section 2 describes our proposed data variation robust learning model based on importance sampling and the algorithm to solve it. The relationship between LogISloss and p-norm is also revealed in this section. In Section 3, we apply the proposed model to the face verification problem. Section 4 shows the experiment results on RFW datasets. Specifically, Section 4.1 introduces datasets including training datasets, testing datasets and the training schedule in the experiments. Section 4.2 analyze the temperature T in LogISloss. Section 4.3 compares ArcLoss and IS-ArcLoss, AddLoss and IS-AddLoss with respect to distribution deviations. Section 4.4 compares ArcLoss and IS-ArcLoss with respect to hard examples. Finally, we conclude this paper in Section 5.

2. Importance sampling based robust risk minimization

In the learning problem considered in this paper, we have training data x_1, x_2, \dots, x_N which are generated i.i.d according to some (usually unknown) probability density function $q(x)$ and a set of loss function $L(x, \omega)$, and we do not know the future data distribution and no future data is available for the leaning system. Our aim is to construct a learning algorithm for a population with unknown distribution $p(x)$. We further assume that if $p(x)$ are, instead of being completely unknown, restricted to a class of distributions, i.e.

$$\Gamma = \{p(x) : KL(p(x) \parallel q(x)) = \int p(x) \log \left(\frac{p(x)}{q(x)} \right) dx \leq C\}. \quad (1)$$

Therefore, our goal becomes to minimize the worst-case expected loss over Γ . A *minimax* approach is applied through minimizing the worst-case loss restricted to this constraint. Section 2.1 gives out the principled deviation of the minimax approach and solves the corresponding optimization problem. Section 2.2 presents the model *LogISloss* under the logarithmic transformation of $L(x, \omega)$ and reveals its relationship with p-norm.

2.1. Principle of ISloss

The performance of a learning system for a given distribution $p(x)$ is measured by the following the risk functional

$$R(\omega) = \int_x L(x, \omega) p(x) dx. \quad (2)$$

First, since we don't know exactly the future data distribution $p(x)$ in Γ , we need to find a $p(x)$ that maximizes the objective function. As $p(x)$ is unknown in the problem, we assume that $p(x)$ subject to the following constraint, $KL(p(x) \parallel q(x)) \leq C$. Therefore, the optimization problem becomes

$$\begin{aligned} \max_{p(x)} \quad & R(\omega) = \int_x L(x, \omega) p(x) dx \\ \text{s.t.} \quad & KL(p(x) \parallel q(x)) \leq C. \end{aligned} \quad (3)$$

Second, given the worst-case distribution $p(x)$, we aim to find the ω which minimizes $R(\omega)$. Then the corresponding optimization problem becomes

$$\begin{aligned} \min_{\omega} \max_{p(x)} \quad & R(\omega) = \int_x L(x, \omega) p(x) dx \\ \text{s.t.} \quad & KL(p(x) || q(x)) \leq C. \end{aligned} \quad (4)$$

In typical statistical learning approach, we usually assume that $p(x) = q(x)$ and use Empirical Risk Minimization[19](ERM in abbreviated form) to train the models, in which the empirical risk is defined as

$$R_E = \frac{1}{N} \sum_{i=1}^N L(x_i, \omega) \quad (5)$$

where the subscript E represents *empirical*. Next, we derive the empirical estimation of the risk functional and KL-divergence using the idea of importance sampling[4, 18, 15] method where a mathematical expectation with respect to $p(x)$ is approximated by a weighted average of random draws from another distribution $q(x)$. For any probability density $q(x)$ with $q(x) > 0$ whenever $p(x) > 0$, the risk functional is

$$R(\omega) = \int_x L(x, \omega) p(x) dx = \int_x L(x, \omega) \frac{\frac{p(x)}{q(x)}}{\int_x \frac{p(x)}{q(x)} q(x) dx} q(x) dx, \quad (6)$$

and the KL-divergence between $p(x)$ and $q(x)$ is

$$KL(p(x) || q(x)) = \int_x p(x) \log \left(\frac{p(x)}{q(x)} \right) dx = \int_x \frac{\frac{p(x)}{q(x)}}{\int_x \frac{p(x)}{q(x)} q(x) dx} \log \left(\frac{\frac{p(x)}{q(x)}}{\int_x \frac{p(x)}{q(x)} q(x) dx} \right) q(x) dx. \quad (7)$$

Then, we derive the empirical estimation of $R(\omega)$ and $KL(p(x) || q(x))$. Suppose the observed dataset $D = \{x_1, x_2, \dots, x_N\}$ are N i.i.d samples drawn from $q(x)$. The self-normalized importance sampling weight for data point x_i is $w_i = w(x_i) = \frac{\frac{p(x_i)}{q(x_i)}}{\frac{1}{N} \sum_{j=1}^N \frac{p(x_j)}{q(x_j)}}$. $\sum_{i=1}^N w_i = 1$ and $W = [w_i]_{N \times 1}$ is called the importance sampling weight distribution. Therefore, the empirical estimation of (6) is,

$$R_E(\omega) = \frac{1}{N} \sum_{i=1}^N \frac{\frac{p(x_i)}{q(x_i)}}{\frac{1}{N} \sum_{j=1}^N \frac{p(x_j)}{q(x_j)}} L(x_i, \omega) = \sum_{i=1}^N L(x_i, \omega) w_i \quad (8)$$

and the empirical estimation of (7) is,

$$\begin{aligned}
KL_E(p(x) \parallel q(x)) &= \frac{1}{N} \sum_{i=1}^N \frac{\frac{p(x_i)}{q(x_i)}}{\frac{1}{N} \sum_{j=1}^N \frac{p(x_j)}{q(x_j)}} \log \frac{\frac{p(x_i)}{q(x_i)}}{\frac{1}{N} \sum_{j=1}^N \frac{p(x_j)}{q(x_j)}} \\
&= \sum_{i=1}^N \frac{\frac{p(x_i)}{q(x_i)}}{\sum_{j=1}^N \frac{p(x_j)}{q(x_j)}} \left(\log \left(\frac{\frac{p(x_i)}{q(x_i)}}{\sum_{j=1}^N \frac{p(x_j)}{q(x_j)}} \right) - \log \frac{1}{N} \right) \\
&= \sum_{i=1}^N w_i \log \frac{w_i}{\frac{1}{N}} = KL(w_i \parallel \{\frac{1}{N}\}) \\
&= \sum_{i=1}^N w_i \log w_i + \log N
\end{aligned} \tag{9}$$

where $\{\frac{1}{N}\}$ denotes the discrete uniform distribution with N samples. Plugging (8) and (9) back into (4), the optimization problem becomes

$$\min_{\omega} \max_W R_E(\omega, W) = \sum_{i=1}^N L(x_i, \omega) w_i, \tag{10}$$

$$\text{s. t. } \sum_{i=1}^N w_i \log w_i + \log(N) \leq C, \tag{11}$$

$$\sum_{i=1}^N w_i = 1, w_i \in [0, 1], \quad 1 \leq i \leq N. \tag{12}$$

where (12) is the constraint for the importance sampling weight W . As a result, the constrained optimization problem in (10) can be reformulated to the unconstrained optimization problem using the Lagrange method. Let the Lagrange multiplier for (11) and (12) to be T and λ respective. The max problem in (10) can be reformulated as

$$F_0(\omega, W) = \sum_{i=1}^N L(x_i, \omega) w_i - T \sum_{i=1}^N w_i \log w_i - T \log(N) - \lambda \left(\sum_{i=1}^N w_i - 1 \right). \tag{13}$$

Here $T > 0$ is the temperature that governs the level of randomness of W . When $T \rightarrow \infty$, the allowed distribution shift $KL(p(x) \parallel q(x))$ should be small while for $T \rightarrow 0$, the distribution shift can be very large. Since T is a predefined hyperparameter, $T \log(N)$ is a constant and can be omitted and finally we get $F(\omega, W)$, which is

$$F(\omega, W) = \sum_{i=1}^N L(x_i, \omega) w_i - T \sum_{i=1}^N w_i \log w_i - \lambda \left(\sum_{i=1}^N w_i - 1 \right). \tag{14}$$

Setting the derivative of $F(\omega, W)$ with respect to w_i to zero, we get the optimality necessary condition for w_i , which is

$$w_i = \frac{\exp(\frac{L(x_i, \omega)}{T})}{\sum_{j=1}^N \exp(\frac{L(x_j, \omega)}{T})}. \quad (15)$$

Substituting (15) back into (14), we get the effective loss functional

$$F^*(\omega) = T \log\left(\sum_{i=1}^N \exp\left(\frac{L(x_i, \omega)}{T}\right)\right). \quad (16)$$

Minimization of $F^*(\omega)$ with respect to ω is equivalent to min-max of $R_E(\omega, W)$ with respect to ω, W .

2.2. LogISloss

In this section, we propose the model under the logarithmic transformation of $L(x, \omega)$ and the resulting model is denoted as LogISloss. The logarithmic risk functional is

$$R_{log}(\omega) = \int_x \log L(x, \omega) p(x) dx. \quad (17)$$

The corresponding optimization problem of LogISloss is

$$\begin{aligned} \min_{\omega} \max_{p(x)} \quad & R_{log}(\omega) = \int_x \log L(x, \omega) p(x) dx \\ \text{s.t.} \quad & KL(p(x) || q(x)) \leq C. \end{aligned} \quad (18)$$

Similar in ISloss, the empirical estimation of the Lagrange of LogISloss is as follows

$$F_{log}^*(\omega) = \log\left(\sum_{i=1}^N L(x_i, \omega)^{\frac{1}{T}}\right)^T. \quad (19)$$

Equation (19) shows that the minimization problem of the logarithmic version F^* is equivalent to minimization of the p-norm loss function with $p = \frac{1}{T}$. The objective function of ISloss(16) involves exponential and not stable in training, therefore we use LogISloss(19) in subsequent experiments.

3. Face Verification

In this section, we apply our proposed LogISLoss to two widely used large-margin softmax variants in face verification task, namely ArcMargin[2] and AddMargin[22]. We denote the loss function under ArcMargin and AddMargin as *ArcLoss* and *AddLoss* and the importance sampling variants of ArcLoss and AddLoss as *IS-ArcLoss* and *IS-AddLoss*. It should be noted that the proposed ISLoss and LogISLoss can be adopted to any loss functions based on each specific learning problem. Here we adopt the proposed model to cross-entropy loss as an example.

3.1. Preliminaries

To begin with, let us retrospect the formulation of ArcMargin and AddMargin. First, we introduce some notations to facilitate the discussion in this section. Suppose N is the number of training samples and C is the number of classes. $x_i \in \mathcal{R}^d$ denotes the deep feature of i -th sample. For x_i , we refer y_i as the target class and j as the non-target class (the label excluding the ground truth one). $W_j \in \mathcal{R}^d$ denotes the j -th column of the weight $W \in \mathcal{R}^{d \times C}$ and $b_j \in \mathcal{R}^C$ is the bias term. We fix bias $b_j = 0$ for simplicity. Suppose $\theta_{j,i}$ is the angle between W_j and x_i . Following [2, 22], we fix the weight $\|W_j\| = 1$ by l_2 normalization and fix the deep feature $\|x_i\|$ by l_2 normalization and rescale it to s . We set the feature scale s to 64 following [2, 22].

ArcLoss ArcFace(Additive Angular Margin Loss)[2] uses the arc-cosine function to calculate the angle between the feature x_i and the target weight W_{y_i} . The model adds an additive angular margin m to the *target angle* to enhance the inter-class discrepancy and intra-class compactness. The ArcLoss for the i -th sample is defined as follows

$$L_i^{Arc} = -\log \frac{e^{s(\cos(\theta_{y_i,i}+m))}}{e^{s(\cos(\theta_{y_i,i}+m))} + \sum_{j=1, j \neq y_i}^C e^{s\cos(\theta_{j,i})}}. \quad (20)$$

AddLoss AddMargin(Additive margin)[20], also known as the Large-Margin Cosine Loss[22], calculates the angle between the feature x_i and the target weight W_{y_i} . The model minus an additive margin m to the cosine of the target angle to maximize inter-class variance

and minimize intra-class variance. The AddLoss for the i -th sample is defined as follows

$$L_i^{Add} = -\log \frac{e^{s(\cos(\theta_{y_i,i})-m)}}{e^{s(\cos(\theta_{y_i,i})-m)} + \sum_{j=1, j \neq y_i}^C e^{s\cos(\theta_{j,i})}} \quad (21)$$

3.2. IS-ArcMargin and IS-AddMargin

Suppose L_i^{Arc} denote ArcLoss for the i -th sample, and n denote the number of samples in each training batch, then IS-ArcLoss is defined as follows

IS-ArcLoss

$$L_{Arc}^{IS} = \log\left(\sum_{i=1}^n (L_i^{Arc})^{\frac{1}{T}}\right)^T. \quad (22)$$

Here, the superscript *IS* denotes **I**mportance **S**ampling. In subsequent experiments for ArcLoss and IS-ArcLoss, the angular margin penalty m is fixed to 0.5 as recommended by [2]. Suppose L_i^{Add} denote the AddLoss for the i -th sample, then IS-AddLoss is defined as follows

IS-AddLoss

$$L_{Add}^{IS} = \log\left(\left\{\sum_{i=1}^n (L_i^{Add})^{\frac{1}{T}}\right\}\right)^T. \quad (23)$$

In subsequent experiments for AddLoss and IS-AddLoss, the additive margin m is fixed to 0.35 as recommended by [22].

4. Experiment

In the face verification task, the training stage is used to learn a deep feature embedding for a given image through a classification task. In the testing stage, the score of a given pair is usually calculated by the cosine similarity between the two feature embeddings. If the score is higher than the verification threshold, the input pair is considered a positive pair. If the score is lower than the verification threshold, the input pair is considered a negative pair. The verification threshold is obtained from cross-validation by a pre-defined split in test datasets.

Table 1: Statistics for BUPT-Equalizedface Dataset. BUPT-Equalizedface is a combination of RFW-Caucasian, RFW-African, RFW-Asian and RFW-Indian.

Dataset	# of ID	# of images
RFW-Caucasian	7000	326484
RFW-African	7000	324376
RFW-Asian	7000	325493
RFW-Indian	6999	275063
BUPT-Equalizedface	27999	1251416

4.1. Datasets

Training Datasets In this paper, we use Racial Faces in-the-Wild(RFW) database[25, 26, 23, 11, 24], which includes four races, namely Caucasian, African, Asian and Indian. We use BUPT-Equalizedface[25] as the training dataset in this paper. BUPT-Equalizedface Dataset has 27999 individuals and 1251416 images in total, the number of individuals in Caucasian, African, Asian and Indian are 7000, 7000, 7000 and 6999 respectively. The detailed statistics of BUPT-Equalizedface are given in Table 1. In later discussions, the four subsets in BUPT-Equalizedface are denoted as RFW-Caucasian, RFW-African, RFW-Asian and RFW-Indian.

Testing Datasets The RFW database has four testing subsets, namely Caucasian, African, Asian and Indian. The abovementioned four races contain 2958, 2995, 2492, 2984 individuals and 10196, 10415, 9688, 10308 images respectively. There are about 14K positive pairs and 50M negative pairs[25] for each subset in RFW-test, most of which are easy to distinguish. The proposed *LogISLoss* aims to highlight large distribution deviations or hard examples. Therefore, we use **RFW-test** for evaluation, which is composed of difficult pairs selected based on cosine similarity between embeddings of each pair[25]. Each subset(race) contains 3000 positive pairs and 3000 negative pairs, split into 10 subsets in advance. We select the verification threshold for one split based on the remaining nine splits. Meta statistics of RFW-test are shown in Table 2. We propose RFW-extend as an extension to RFW-test and the details of the dataset are in Section 4.4. Figure 1

Table 2: Statistics for testing datasets.

Dataset	# of positive pairs	# of negative pairs	# of total pairs
Caucasian	3000	3000	6000
African	3000	3000	6000
Asian	3000	3000	6000
Indian	3000	3000	6000
Caucasian-extend(proposed)	13650	42260	55910
African-extend(proposed)	14050	43370	57420
Asian-extend(proposed)	15690	54890	70580
Indian-extend(proposed)	13860	43120	56980

shows selected positive pairs and negative pairs from each subset. It can be seen that some pairs are difficult even for human observers.

Experiment Settings The datasets are aligned and preprocessed in MXNet binary format and the size of the cropped image is set to 112×112 . We set the training batch size, weight decay and momentum as 128, $5e-4$ and 0.9, respectively. The dimension of embedding feature is set to 512 following [9, 22, 28, 2]. The initial learning rate is set to 0.1, and decreased by a factor of 10 at given epochs. For BUPT-Equalizedface dataset, we train the network for 27 epochs and decay the learning rate at epoch 14, 20 and 24. We use half of the suggested epochs in [26] to save training time. We use IResNet-34[2], a 34-layer modified ResNet, as the default backbone in all experiments if not otherwise specified. We follow the Pytorch implementation of insightface¹ on one GTX 1080ti and one GTX 3090ti for training.

4.2. Temperature

The proposed model has a hyperparameter T which implicitly controls the allowed distribution deviations. In this section, we analyze how the temperature T affects the model

¹https://github.com/deepinsight/insightface/tree/master/recognition/arcface_torch

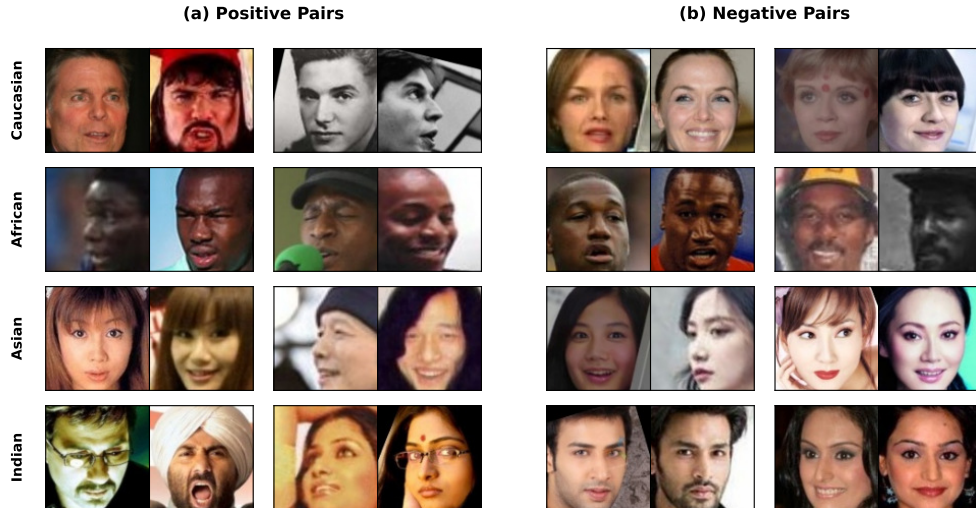


Figure 1: Images from RFW-test. Four rows show examples from Caucasian, African, Asian and Indian respectively. (a) shows hard positive pairs and (b) shows hard negative pairs.

performance. When $T \rightarrow \infty$, the allowed distribution shift $KL(p(x) \parallel q(x))$ should be small while for $T \rightarrow 0$, the distribution shift can be very large. Figure 2 compares verification accuracy on four test datasets when $T = 0.3, 0.5, 0.7, 0.9$. The model was trained on RFW-Caucasian using IS-ArcLoss. Figure 2 shows that $T = 0.5$ achieves the best accuracy on African, Asian and Indian while $T = 0.7$ achieves the best accuracy on Caucasian. One possible reason is that the distribution deviation between RFW-Caucasian (training) and Caucasian(testing) is smaller than the distribution deviation between RFW-Caucasian (training) and African/Asian/Indian(testing), therefore, the testing Caucasian favors a higher temperature, $T = 0.7$. This observation validates our assumption that lower T tolerates larger distribution deviation. In this paper, we use a fixed $T = 0.5$ as the default temperature in all subsequent experiments. However, other training schedule on T can be adopted. For example, start training at a high temperature and decaying it during training. How to choose a good schedule of T in different learning problems will be explored in our future study.

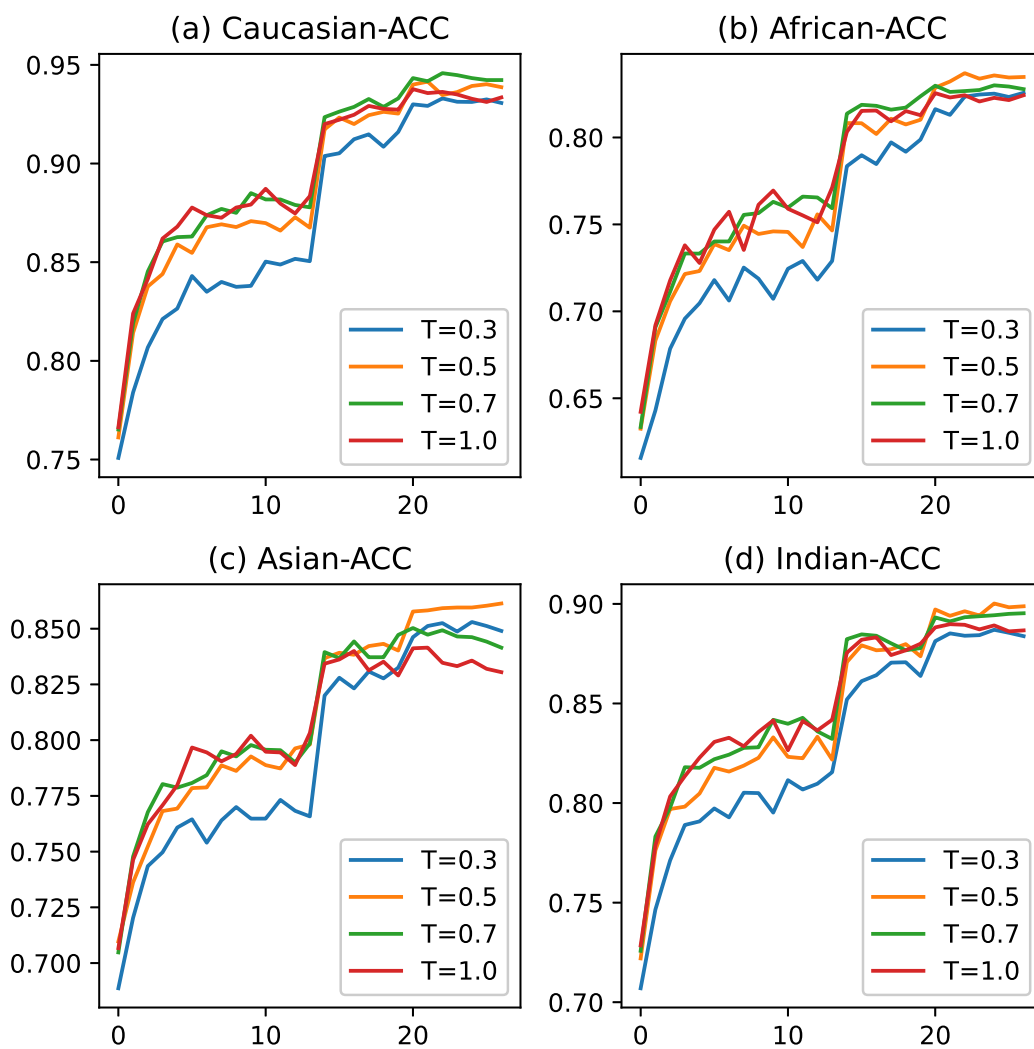


Figure 2: Comparison of verification accuracy among different T on IS-ArcLoss. X-axis represents training epochs while Y-axis represents verification accuracy. The model was trained on RFW-Caucasian.

Table 3: Verification accuracy(%) of IResNet-34 models trained on four datasets. Results are in % and higher number indicates better performance.

Train	Loss	Caucasian	African	Asian	Indian
RFW-Caucasian	ArcLoss	93.55	82.23	84.70	88.77
	IS-ArcLoss	94.15(0.60)	83.22(0.99)	85.82(1.12)	89.40(0.63)
RFW-African	ArcLoss	89.23	92.37	84.02	88.20
	IS-ArcLoss	90.37(1.14)	92.43(0.06)	85.82(1.80)	89.65(1.45)
RFW-Asian	ArcLoss	85.50	79.13	90.90	84.45
	IS-ArcLoss	87.20(1.70)	80.30(1.17)	91.17(0.27)	85.32(0.87)
RFW-Indian	ArcLoss	87.98	81.47	83.60	91.50
	IS-ArcLoss	88.92(0.94)	82.30(0.83)	83.48(-0.12)	91.80(0.30)

4.3. LogISloss

In this section, we compare experiment results on both ArcMargin and AddMargin. Table 3 and Table 4 compares verification accuracy on ArcMargin and AddMargin respectively, Table 5 shows TAR@FAR of different models and Figure 3 draws ROC, DET and ACC curves on four RFW-test subsets. Table 6 compares results on other standard face verification test datasets. Table 7 compares models under different backbones.

Table 3 compares verification accuracy between ArcLoss and IS-ArcLoss. The models are trained on RFW-Caucasian, RFW-African, RFW-Asian, RFW-Indian and tested on Caucasian, African, Asian, Indian. We report the result at the epoch where the training race has the highest accuracy. The accuracy gain(small brackets) is the difference of our proposed IS-ArcLoss over ArcLoss. For example, the model trained on RFW-Caucasian and tested on African achieves 82.23% verification accuracy under ArcLoss and 83.22% verification accuracy under IS-ArcLoss, the accuracy gain is 0.99%. Table 3 shows the following findings. First, IS-ArcLoss performs better than ArcLoss in most cases. One exception is the model trained on RFW-Indian and tested on Asian, which observes a little performance drop(-0.12%). Second, the accuracy gains on different races are higher compared with the training race itself on three test datasets(RFW-Caucasian, RFW-African,

Table 4: Verification accuracy(%) of IResNet-34 models trained on different training dataset.

Train	Loss	Caucasian	African	Asian	Indian
RFW-Caucasian	AddLoss	94.28	83.27	85.70	89.45
	IS-AddLoss	93.68(-0.60)	83.07(-0.20)	85.97(0.27)	89.68(0.23)
RFW-African	AddLoss	90.85	92.72	84.85	89.85
	IS-AddLoss	89.98(-0.87)	92.50(-0.22)	86.10(1.25)	89.93(0.08)
RFW-Asian	AddLoss	86.75	79.62	91.17	85.22
	IS-AddLoss	86.87(0.12)	80.63(1.01)	90.28(-0.89)	85.75(0.53)
RFW-Indian	AddLoss	88.93	82.78	83.93	92.13
	IS-AddLoss	88.47(-0.46)	82.12(-0.66)	83.02(-0.91)	91.20(-0.93)

RFW-Asian). Take the models trained on RFW-Caucasian(first row) for example, the accuracy gain on Caucasian, African, Asian, Indian is 0.6%, 0.99%, 1.12% and 0.63% respectively. The accuracy gain on Caucasian(0.6%) is the lowest. This observation indicates that IS-ArcLoss has a better generalization ability compared with ArcLoss. Third, considering the model trained on RFW-African(second row), the test accuracy on Asian, Indian and Caucasian is 84.02%, 88.20% and 89.23%. The distribution of training data is deviated from the distribution of test data. If we assume the accuracy gap is a measure of the distribution shift, then a larger accuracy gap indicates a larger distribution shift. Under this assumption, the distribution deviations between Asian, Indian, Caucasian and African are in increasing order. The accuracy gain of the three datasets is 1.80%, 1.45% and 1.14%, which is in decreasing order. This observation implies that the proposed IS-ArcLoss performs better when the distribution deviation is large.

Table 4 compares verification accuracy between AddLoss and IS-AddLoss. IS-AddLoss performs better than AddLoss on 3(RFW-Caucasian, RFW-African, RFW-Asian) out of 4 datasets with respect to the generalization ability of different races. Another interesting observation is in line with the observations from Table 3. For the models trained on RFW-African, the accuracy gain on Asian(84.85%), Indian(89.85%) and Caucasian(90.85%) is 1.25%, 0.08% and -0.87%, which is in decreasing order. For the models trained on RFW-

Table 5: Comparison of TAR at given FAR. “Arc” represents “ArcLoss” and “IS-Arc” represents “IS-ArcLoss”.

Train	Method	Caucasian			African			Asian			Indian		
FAR		1e-1	1e-2	1e-3	1e-1	1e-2	1e-3	1e-1	1e-2	1e-3	1e-1	1e-2	1e-3
R-Ca	Arc	94.70	83.77	73.50	72.40	41.10	22.03	78.23	54.33	37.70	87.53	64.43	49.60
	IS-Arc	95.37	84.63	70.00	76.61	44.20	20.33	80.43	54.03	34.43	88.50	68.10	50.63
R-Af	Arc	88.20	69.00	49.40	92.00	73.03	55.60	77.60	47.30	30.63	87.63	65.33	51.17
	IS-Arc	90.33	66.87	49.77	92.93	78.80	63.87	80.93	55.00	37.90	89.33	68.00	50.93
R-As	Arc	82.16	55.47	27.00	66.80	38.27	22.77	90.47	74.37	55.10	80.00	50.27	29.67
	IS-Arc	84.10	60.77	39.13	68.00	40.63	19.67	91.27	75.73	55.73	81.67	55.70	31.37
R-Id	Arc	85.97	64.17	43.50	71.53	42.80	24.00	77.13	49.67	29.10	91.37	74.77	61.57
	IS-Arc	88.13	65.17	45.97	72.67	46.10	28.00	76.93	48.27	32.60	91.67	78.13	60.27

Asian, the accuracy gain on African(79.62%), Indian(85.22%) and Caucasian(86.75%) is 1.01%, 0.53% and 0.12%, which is in decreasing order. These also validate our findings in Table 3 that IS-AddLoss performs better when the distribution shift is large.

Table 5 compares True Acceptance Rate(TAR) at given False Acceptance Rate(FAR), (1e-1, 1e-2, 1e-3) between ArcLoss and IS-ArcLoss. TAR@FAR in Table 5 is calculated following [8]. Table 5 shows that IS-ArcLoss yields a performance boosts on true acceptance rate on 8, 10, 11 and 10 out of 12 compared results in four test races respectively.

In Figure 3, three metrics are adopted to compare the performance between ArcLoss and IS-ArcLoss. The model was trained on RFW-Caucasian, RFW-Asian, RFW-Indian and tested on African. We use African as the test dataset since it has the lowest accuracy among the four races in Table 3 and Table 4. The first column in Figure 3 shows the Receiver Operating Characteristic(ROC) curve, which is false positive rate against true positive rate(closer to the top left, the better). The second column in Figure 3 shows the Detection Error Trade-off curves(DET)[16], which is false positive rate against false negative rate(closer to the bottom left, the better). The third column in Figure 3 shows the accuracy curve, which is false positive rate against accuracy(the higher, the better).

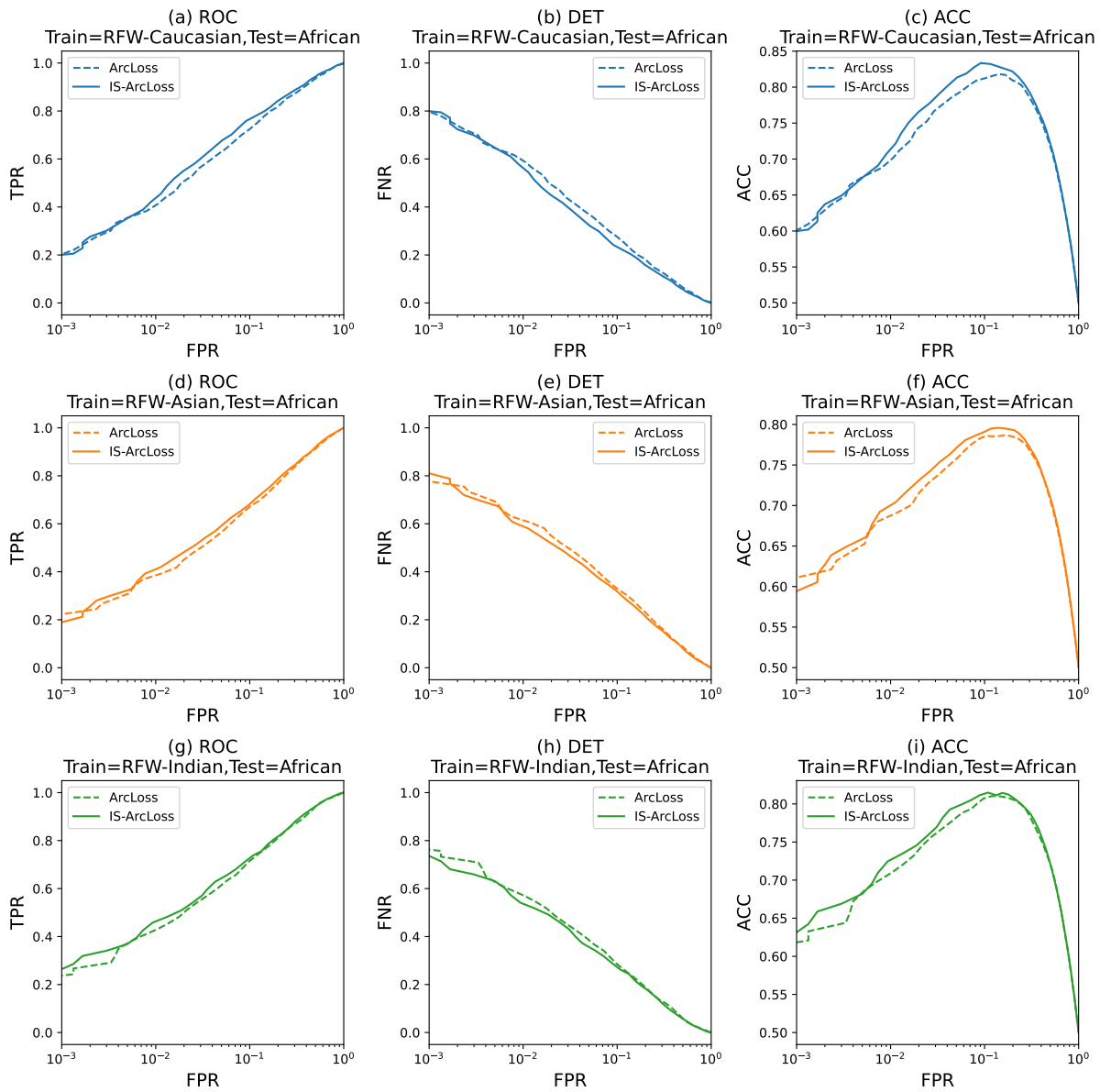


Figure 3: ROC,DET and ACC curves between ArcLoss and IS-ArcLoss.

Table 6: Verification accuracy(%) of IResNet-34 models trained on different training datasets. “Arc” represents “ArcLoss” and “IS-Arc” represents “IS-ArcLoss”. “R-Ca, R-Af, R-As, R-Id” represents “RFW-Caucasian, RFW-African, RFW-Asian, RFW-Indian” respectively.

Train	Loss	LFW	CFP-FP	CFP-FF	AgeDB	CALFW	CPLFW
R-Ca	Arc	99.30	86.39	98.90	94.67	92.28	84.40
	IS-Arc	99.33(0.03)	88.41(2.02)	99.11(0.21)	95.47(0.80)	92.87(0.59)	84.90(0.50)
R-Af	Arc	99.12	86.03	98.77	90.68	91.37	82.82
	IS-Arc	99.10(-0.02)	87.09(1.06)	98.97(0.20)	92.20(1.52)	91.77(0.40)	83.62(0.80)
R-As	Arc	98.13	89.46	97.49	89.55	88.42	82.65
	IS-Arc	98.62(0.49)	91.51(2.05)	97.37(-0.12)	90.30(0.75)	89.28(0.86)	83.17(0.52)
R-Id	Arc	98.62	92.30	98.27	89.28	89.32	84.93
	IS-Arc	98.68(0.06)	92.53(0.23)	98.41(0.14)	90.77(1.49)	89.42(0.10)	85.57(0.64)

Results in Figure 3 show that IS-ArcLoss generalizes better than ArcLoss under different evaluation metrics.

Table 6 test LogISloss on several popular benchmarks, including Labeled Faces in the Wild(LFW)[5], Age-DB[12], Cross-age LFW(CALFW)[31], Cross-pose LFW(CPLFW)[30] and Celebrities in Frontal-Profile (CFP-FP and CFP-FF)[17], where LFW, AGE-DB, CALFW, CPLFW have 6000 pairs and CFP(large pose variation) has 7000 pairs. These datasets are also split into 10 subsets in advance. The results are evaluated on the final epoch(epoch=27). Table 6 shows that IS-ArcLoss performs better than ArcLoss in most cases. Especially, the accuracy gains on LFW and CFP-FF are low, the accuracy gains on CALFW and CPLFW are medium, and the accuracy gains on CFP-FP and AgeDB are high.

Table 7 compares IS-ArcLoss and ArcLoss under different backbones trained on RFW-Caucasian dataset. The initial learning rate for MobileFaceNet² is set to 0.05 since ArcLoss encounters NaNs if the initial learning rate is set to 0.1. The total training epoch

²<https://github.com/cavalleria/cavaface>

Table 7: Verification accuracy(%) of different backbones. The models are trained on RFW-Caucasian dataset.

Train	Loss	Caucasian	African	Asian	Indian
MobileFaceNet	ArcLoss	91.80	80.27	83.40	86.87
	IS-ArcLoss	91.98(0.18)	80.37(0.10)	83.67(0.27)	87.37(0.50)
IResNet-100	ArcLoss	94.82	83.92	85.73	89.63
	IS-ArcLoss	95.67(0.85)	85.43(1.51)	86.65(0.92)	90.72(1.09)

for IResNet-100 is set to 35 since it is a deep CNN model. Table 7 shows that IS-ArcLoss performs better than ArcLoss using the lightweight MobileFaceNet[1] and deep network like IResNet-100.

4.4. Hard Pairs

RFW-test-extend Dataset Since RFW-test only has 6000 pairs for each race, in this experiment, we propose an extended test dataset RFW-test-extend to include more pairs for evaluation. In RFW-test-extend, the positive pairs are collected from each individual’s all available images in RFW-test. The negative pairs are collected from combinatorial pairs of each individual’s hard negatives individuals. The hard negative individuals are from the meta data of RFW-test, which means two individuals from RFW-test’s negative pair are considered as a hard individual for each other. All positive pairs and negative pairs are randomly split into 10 folds as RFW-test. The statistics for RFW-extend are shown in Table 2.

In face verification problem, for positive pairs, the similarity between two images should be high, therefore **hard positive** pairs have low similarity. For negative pairs, the similarity between two images should be low, therefore **hard negative** pairs have high similarity. Figure 4 shows the similarity of top-100 hard positive and hard negative pairs. The model was trained on the whole BUPT-Equalizedface datasets using ArcLoss. Figure 4 shows that IS-ArcLoss has higher similarity for positive pairs compared with ArcLoss in (a)(Caucasian-extend), (c)(Asian-extend), (d)(Indian-extend) and it has lower similarity

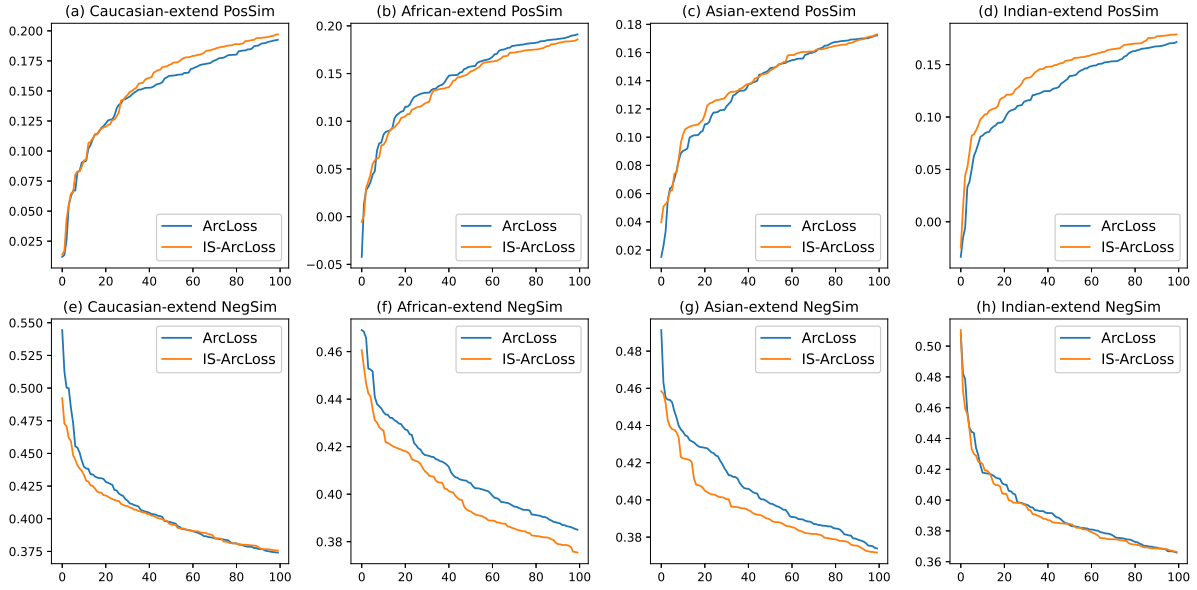


Figure 4: Hard pairs’ similarity comparison between ArcLoss and IS-ArcLoss. The model was trained on RFW-Equalizedface and tested on RFW-test-extend dataset. (a)(b)(c)(d) show positive similarity while (e)(f)(g)(h) show negative similarity.

for negative pairs in all four tested datasets. Visualization of the top-2 hardest pairs for each race is shown in Figure 1. This observation indicates that IS-ArcLoss highlights the hardest pairs.

5. Conclusion

In this paper, we proposed an importance sampling based data variation robust learning method (IS-DVR) to solve the problem of data distribution deviation between current training data and future testing data. The objective function of IS-DVR is derived from an information-theoretical viewpoint and we reveal that minimization of the objective function of LogISloss is equivalent to minimization of p-norm loss function when $p = \frac{1}{T}$. We apply the proposed model to the face verification problem and experiment results show that LogISloss generalizes better than cross-entropy loss across different RFW datasets under large distribution deviations. We are currently working on applying ISloss and LogISloss to other machine learning problems and how to design the temperature T is not clear and remains to be explored in future endeavour.

Disclosure statement

No potential conflict of interest was reported by the authors.

Acknowledgements This work is supported by the National Natural Science Foundation of China under Grants 61976174.

References

- [1] Chen, S., Liu, Y., Gao, X., and Han, Z. (2018). Mobilefacenet: Efficient cnns for accurate real-time face verification on mobile devices. In *Biometric Recognition: 13th Chinese Conference, CCBR 2018, Urumqi, China, August 11-12, 2018, Proceedings 13*, pages 428–438. Springer.
- [2] Deng, J., Guo, J., Xue, N., and Zafeiriou, S. (2019). Arcface: Additive angular margin loss for deep face recognition. In *Proceedings of the IEEE/CVF conference on computer vision and pattern recognition*, pages 4690–4699.
- [3] Farnia, F. and Tse, D. (2016). A minimax approach to supervised learning. *Advances in Neural Information Processing Systems*, 29.
- [4] Glynn, P. W. and Iglehart, D. L. (1989). Importance sampling for stochastic simulations. *Management science*, 35(11):1367–1392.
- [5] Huang, G. B., Mattar, M., Berg, T., and Learned-Miller, E. (2008). Labeled faces in the wild: A database for studying face recognition in unconstrained environments. In *Workshop on faces in 'Real-Life' Images: detection, alignment, and recognition*.
- [6] Kailath, T. (1967). The divergence and bhattacharyya distance measures in signal selection. *IEEE transactions on communication technology*, 15(1):52–60.
- [7] Kullback, S. and Leibler, R. A. (1951). On information and sufficiency. *The annals of mathematical statistics*, 22(1):79–86.
- [8] Liu, W., Wen, Y., Raj, B., Singh, R., and Weller, A. (2022). Sphereface revived: Unifying hyperspherical face recognition. *IEEE Transactions on Pattern Analysis and Machine Intelligence*.

- [9] Liu, W., Wen, Y., Yu, Z., Li, M., Raj, B., and Song, L. (2017). Sphereface: Deep hypersphere embedding for face recognition. In *Proceedings of the IEEE conference on computer vision and pattern recognition*, pages 212–220.
- [10] Liu, W., Wen, Y., Yu, Z., and Yang, M. (2016). Large-margin softmax loss for convolutional neural networks. *arXiv preprint arXiv:1612.02295*.
- [11] Masi, I., Wu, Y., Hassner, T., and Natarajan, P. (2018). Deep face recognition: A survey. In *2018 31st SIBGRAPI conference on graphics, patterns and images (SIBGRAPI)*, pages 471–478. IEEE.
- [12] Moschoglou, S., Papaioannou, A., Sagonas, C., Deng, J., Kotsia, I., and Zafeiriou, S. (2017). Agedb: the first manually collected, in-the-wild age database. In *proceedings of the IEEE conference on computer vision and pattern recognition workshops*, pages 51–59.
- [13] Pardo, L. (2018). *Statistical inference based on divergence measures*. Chapman and Hall/CRC.
- [14] Rényi, A. et al. (1961). On measures of entropy and information. In *Proceedings of the fourth Berkeley symposium on mathematical statistics and probability*, volume 1. Berkeley, California, USA.
- [15] Robert, C. P., Casella, G., and Casella, G. (2010). *Introducing monte carlo methods with r*, volume 18. Springer.
- [16] Robinson, J. P., Livitz, G., Henon, Y., Qin, C., Fu, Y., and Timoner, S. (2020). Face recognition: too bias, or not too bias? In *Proceedings of the IEEE/CVF Conference on Computer Vision and Pattern Recognition Workshops*, pages 0–1.
- [17] Sengupta, S., Chen, J.-C., Castillo, C., Patel, V. M., Chellappa, R., and Jacobs, D. W. (2016). Frontal to profile face verification in the wild. In *2016 IEEE winter conference on applications of computer vision (WACV)*, pages 1–9. IEEE.

- [18] Tokdar, S. T. and Kass, R. E. (2010). Importance sampling: a review. *Wiley Interdisciplinary Reviews: Computational Statistics*, 2(1):54–60.
- [19] Vapnik, V. (1999). *The nature of statistical learning theory*. Springer science & business media.
- [20] Wang, F., Cheng, J., Liu, W., and Liu, H. (2018a). Additive margin softmax for face verification. *IEEE Signal Processing Letters*, 25(7):926–930.
- [21] Wang, F., Xiang, X., Cheng, J., and Yuille, A. L. (2017). Normface: L2 hypersphere embedding for face verification. In *Proceedings of the 25th ACM international conference on Multimedia*, pages 1041–1049.
- [22] Wang, H., Wang, Y., Zhou, Z., Ji, X., Gong, D., Zhou, J., Li, Z., and Liu, W. (2018b). Cosface: Large margin cosine loss for deep face recognition. In *Proceedings of the IEEE conference on computer vision and pattern recognition*, pages 5265–5274.
- [23] Wang, M. and Deng, W. (2020). Mitigating bias in face recognition using skewness-aware reinforcement learning. In *Proceedings of the IEEE/CVF conference on computer vision and pattern recognition*, pages 9322–9331.
- [24] Wang, M. and Deng, W. (2021). Deep face recognition: A survey. *Neurocomputing*, 429:215–244.
- [25] Wang, M., Deng, W., Hu, J., Tao, X., and Huang, Y. (2019). Racial faces in the wild: Reducing racial bias by information maximization adaptation network. In *Proceedings of the IEEE/CVF International Conference on Computer Vision (ICCV)*.
- [26] Wang, M., Zhang, Y., and Deng, W. (2021). Meta balanced network for fair face recognition. *IEEE Transactions on Pattern Analysis and Machine Intelligence*, pages 1–1.
- [27] Wang, X., Zhang, S., Wang, S., Fu, T., Shi, H., and Mei, T. (2020). Mis-classified vector guided softmax loss for face recognition. In *Proceedings of the AAAI Conference on Artificial Intelligence*, volume 34, pages 12241–12248.

- [28] Wen, Y., Zhang, K., Li, Z., and Qiao, Y. (2016). A discriminative feature learning approach for deep face recognition. In *Computer Vision—ECCV 2016: 14th European Conference, Amsterdam, The Netherlands, October 11–14, 2016, Proceedings, Part VII 14*, pages 499–515. Springer.
- [29] Williams, P. M. (1980). Bayesian conditionalisation and the principle of minimum information. *The British Journal for the Philosophy of Science*, 31(2):131–144.
- [30] Zheng, T. and Deng, W. (2018). Cross-pose lfw: A database for studying cross-pose face recognition in unconstrained environments. *Beijing University of Posts and Telecommunications, Tech. Rep*, 5:7.
- [31] Zheng, T., Deng, W., and Hu, J. (2017). Cross-age lfw: A database for studying cross-age face recognition in unconstrained environments. *arXiv preprint arXiv:1708.08197*.